



Gedunin isolated from the mangrove plant *Xylocarpus granatum* exerts its anti-proliferative activity in ovarian cancer cells through G2/M-phase arrest and oxidative stress-mediated intrinsic apoptosis

Rohit Sahai¹ · Arindam Bhattacharjee¹ · Vishwa Nath Shukla² · Pragya Yadav^{2,4} · Mohammad Hasanain^{3,4} · Jayanta Sarkar^{3,4} · T. Narender^{2,4} · Kalyan Mitra^{1,4}

Published online: 13 May 2020
© Springer Science+Business Media, LLC, part of Springer Nature 2020

Abstract

Gedunin is a natural tetranortriterpenoid secondary metabolite found in plants of the Meliaceae family, which has been reported for its antiparasitic, antifungal and anticancer activities. Here, we describe the molecular mechanisms underlying the in vitro anti proliferative activity of gedunin (isolated from the mangrove plant *Xylocarpus granatum*) in human ovarian cancer cells. We observed that gedunin triggered severe ROS generation leading to DNA damage and cell cycle arrest in G2/M phase thus inhibiting cell proliferation. ROS upregulation also led to mitochondrial stress and membrane depolarization, which eventually resulted in mitochondria-mediated apoptosis following cytochrome C release, caspase 9, 3 activation, and PARP cleavage. Transmission electron microscopy of gedunin treated cells revealed sub-cellular features typical of apoptosis. Moreover, an upregulation in stress kinases like phospho-ERK 1/2, phospho-p38 and phospho-JNK was also observed in gedunin treated cells. Free radical scavenger N-Acetyl-L-Cysteine (NAC) reversed all these effects resulting in increased cell survival, abrogation of cell cycle arrest, rescue of mitochondrial membrane potential and suppression of apoptotic markers. Interestingly, gedunin is also an inhibitor of the evolutionarily conserved molecular chaperone Heat Shock Protein 90 (hsp90) responsible for maintaining cellular homeostasis. Targeting this chaperone could be an attractive strategy for developing cancer therapeutics since many oncogenic proteins are also client proteins of hsp90. Collectively, our findings provide insights into the molecular mechanism of action of gedunin, which may aid drug development efforts against ovarian cancer.

Keywords Terpenoid · Anti-cancer · Oxidative stress · G2/M arrest · Intrinsic apoptosis · Electron microscopy

Introduction

Ovarian cancer (OC) ranks 7th among most commonly diagnosed gynecological malignancies among women worldwide [1]. In India, its trends have been observed to be increasing, ranking it 4th common cancer in Indian women [2]. While in US, it is reported to be 2nd most common gynecological cancer [3] with an average 5-year survival rate of 47.6% [4]. The disease commonly presents itself at late stages when survival rate is low, posing therapeutic challenges in medical treatments due to chemo-resistance and advancement in stage of progression [5]. This calls for development of better and sustainable treatment options for management of ovarian cancer.

Naturally sourced molecules like polyphenols [6], alkaloids [7], flavonoids [8] and terpenoids [9] have been reported to be effective in management of various pathologies including cancers, owing to their efficacy, safer toxicity

✉ Kalyan Mitra
k_mitra@cdri.res.in

¹ Electron Microscopy Unit, Sophisticated Analytical Instrument Facility and Research, CSIR – Central Drug Research Institute, Sector-10, Jankipuram Extension, Lucknow, Uttar Pradesh 226 031, India

² Medicinal and Process Chemistry Division, CSIR – Central Drug Research Institute, Sector-10, Jankipuram Extension, Lucknow, Uttar Pradesh 226 031, India

³ Division of Biochemistry, CSIR – Central Drug Research Institute, Sector-10, Jankipuram Extension, Lucknow, Uttar Pradesh 226 031, India

⁴ Academy of Scientific and Innovative Research, Ghaziabad, Uttar Pradesh 201 002, India

profiles and long history of use in traditional medicine. Understanding the molecular mechanism of anticancer agents is crucial for development of chemotherapeutics. Gedunin (GDN) is a tri-terpenoid derived from common Indian subcontinent trees like Neem '*Azadirachita indica*', Cedar Mangrove '*Xylocarpus granatum*' and other members of Meliaceae family [10, 11]. It has been shown to have anti-malarial, insecticidal, anti-cancer activity and found to inhibit pancreatic alpha amylase in vitro [12, 13]. Moreover, gedunin is also involved in modulating T lymphocyte response and ameliorating allergic inflammation [14]. Heat Shock Protein 90 complex (HSP90) is a multimeric chaperone assembly involved in essential cellular processes responsible for maintaining cellular homeostasis. Targeting this chaperone could be an attractive strategy for developing cancer therapeutics since many oncogenic proteins are clients of HSP90. Gedunin has been found to be a HSP90 inhibitor that acts by directly binding p23/PTGES3 (an integral part of the HSP90 machinery) leading to its inactivation [10]. Studies indicate gedunin inhibits proliferation of colon cancer cells, human teratocarcinoma cells, pancreatic cancer and ovarian cancer cells; however detailed molecular mechanisms of its action have not been explored [11, 15–17]. The specificity of gedunin towards cancer cells is also evident since it has not been found to be cytotoxic in both human peripheral blood mononuclear cells (PMBCs) and Vero (ATCC CCL-81) mammalian kidney epithelial cells [15, 18].

Sustaining proliferative signals, evading growth suppression and resisting cell death are among the hallmark features of cancer [19]. A disruptive cell cycle plays an important role in uncontrolled proliferation of cancer cells sidelining the checkpoints [20]. Many of the anti-cancer compounds have been found to stall the cell cycle at one or more checkpoints thus halting the cell division and proliferation. Among other stress inducers, reactive oxygen species (ROS) mainly produced in mitochondrial metabolism is an important factor that is responsible for cellular stress and inhibits cell proliferation by causing DNA damage and cell cycle arrest [21]. These aforesaid cellular stresses when prolonged beyond repair mechanisms can lead to programmed cell death including apoptosis [22].

Here, in this study we attempt to elucidate the molecular mechanisms underlying the anti-proliferative action of gedunin in ovarian cancer cells in vitro. We demonstrate that gedunin induced severe oxidative stress, caused mitochondrial stress and depolarization, G2/M cell cycle arrest, activated stress kinases and inhibited proliferative pathways (JAK-STAT, mTOR) which ultimately results in caspase dependent apoptosis in ovarian cancer cells. An ultrastructural analysis of gedunin treated cells revealed altered mitochondrial morphology and showed distinct features of apoptosis. Overall, our results provide insights into the mechanism of action of gedunin and demonstrate

its potential for developing it as an HSP90 targeting anti-cancer agent.

Material and methods

Isolation of gedunin

5 Kg of powdered epicarp of the fruits of *Xylocarpus granatum* were soaked in 10 L of water-ethanol (50:50) for 24 h and the resultant aqueous-alcoholic extract was collected. This process was repeated for four times. The combined aqueous-alcoholic extract was concentrated using rotary evaporator under reduced pressure to give a dark brown powder (480 g). The aqueous-alcoholic extract was macerated with ethyl acetate solvent and concentrated using rotary evaporator under reduced pressure to give ethyl acetate fraction (45 g). The resultant ethyl acetate fraction was subjected to gross column chromatography with hexane-ethylacetate solvent system. The fractions eluted with hexane-ethyl acetate (70:30 and 60:40) solvent system were pooled and concentrated to give 10.4 g of fraction, which was again subjected to small column chromatography to isolate 1.2 g of gedunin in hexane-ethylacetate (65:35) solvent system and the purity of the compound was monitored by TLC in the hexane-ethyl acetate (60:40) solvent system.

Cell lines

PA-1 (ATCC CRL-1572), OVCAR-3 (ATCC HTB-161)—Human ovarian cancer cells, FaDu (ATCC HTB-43)—Human pharyngeal cancer, SW-620 (ATCC CCL-227)—Human colon cancer and MDA-MB-231 (ATCC HTB-261)—Human breast cancer, A549 (ATCC CCL-185)—Human lung cancer cell lines were obtained from American Type Cell Culture (ATCC, Manassas, VA, USA). The cells were cultured as per ATCC recommendations, generally in DMEM, High glucose (12100061) or RPMI 1640 culture media, buffered with sodium bicarbonate and supplemented with 10% Fetal Bovine Serum (FBS) and Antibiotic-Antimycotic (Sigma 100×) at 37 °C in 5% CO₂.

Reagents and chemicals

DMSO Anhydrous (D12345), CM-H₂DCFDA (C6827), MitoSox (M36008), Hoechst 33342 (H3570), JC-1 (T3168), AlexaFluor 488 conjugated antibodies (A-11094), BCA Protein estimation kit (23227), DMEM—High glucose (12100061), RPMI 1640 (51800035), FBS (10437028) were purchased from Gibco™/Invitrogen™ (Life Technologies)/Pierce™ under Thermo Scientific.

Caspase Inhibitor z-VAD-fmk (627610), protease inhibitor cocktail (539131), phosphatase inhibitor cocktail

(524624), Tris Base (648311) and FluorSave mounting media (345789) were purchased from Merck. FITC Annexin V Apoptosis detection kit (556547) were from BD Pharmingen™. Primary antibodies—cdc25C (4688), p21 Waf1/Cip1 (2947), Phospho-Histone H2A.X (9718), Phospho-p53 (9268), Caspase 3 (9662), Caspase 9 (9502), PARP (9532), Bax (5023), Bcl2(15071), MAPK Family Antibody/ Phospho MAPK Family Antibody Sampler Kits (9926/ 9910), BiP/GRP78 (3177), CHOP (5554), JAK2 (3230), STAT3 (4904), phospho-mTOR (2971); and phospho p42/44 MAPK inhibitor U0126 (9903) were purchased from Cell Signaling Technology. ECL Clarity Substrate (1705061) and PVDF membrane (1620177) were from BioRad.

Antibiotic-Antimycotic (A5955), Trypsin (59418C), Anti- β -actin (A1978), Anti-rabbit HRP (AP307P), Anti-mouse HRP (AP308P) antibodies, N-Acetyl-L-Cysteine (A7250), Carbonyl cyanide 3-chlorophenylhydrazone (C2759), SP600125 (S5567), Doxorubicin (D1515), RNase A(R6513), Bovine Serum Albumin (A2153), PBS tablets (P4417), Sulforhodamine B (230162), Tri-chloro acetic acid (T6399), Triton (X100), Acrylamides (A3553/ M7279), Ammonium Persulphate (A3678), Osmium tetroxide (O5500), glutaraldehyde (G5882), Spurr embedding kit (EM0300), and other chemicals were purchased from Sigma Aldrich.

Cell/drug treatments of gedunin

The tetranortriterpenoid gedunin (chemical structure Fig. 1a) was found to be freely soluble in DMSO at 50 mM stock concentrations, and sparingly soluble in aqueous media. Therefore, for treatment of cells, freshly diluted gedunin was used, with dose dilutions in DMSO corresponding to IC₅₀ values of respective cells as mentioned in result section, while only DMSO served as vehicle control (VC).

Cell viability assay

Cell Viability assay was performed using Sulforhodamine B (SRB) dye [23]. 1×10^4 cells/well were grown in 96-well plate and were treated with indicated dose of gedunin for 48 h. Following treatment, the cells were fixed in ice for 1 h using chilled 50% w/v Trichloro Acetic acid (TCA). Post fixation, the culture plate was washed gently in running water (three times) and air-dried. Fixed cells were stained with 0.5% in SRB (in 1% Acetic acid) and washed three times with 1% v/v acetic acid. Bound SRB crystal were dissolved in 10 mM Tris Base (pH 10) for 1 h and the absorbance of each well was measured at 515 nm using a BioTek™ microplate reader.

In vitro scratch assay

In vitro scratch assay was followed with slight modifications as described in [24]. 1×10^5 cells per well were grown in 6-well plate and allowed to proliferate till ~ 80% confluence was reached. A scratch in the cell monolayer was made across the diameter of the well using a sterile 100 μ l pipette tip, followed by PBS wash to remove detached cells. The images were recorded with an inverted phase contrast microscope. Cells were then subjected to gedunin treatment and allowed to grow till the time the scratch in control wells were healed. This was then compared with the confluence of treatment cells at the same time point respectively. Image J (NIH) software was used to calculate the relative area of cell confluence.

Cell cycle analysis

Flow cytometry based cell cycle analysis using nucleic acid staining methods were performed as described in [25]. Briefly, PA-1 and OVCAR-3 cells were grown to 50% confluence and treated with indicated doses of gedunin for 12 h, 24 and 48 h time points. The treated cells were detached using trypsin and fixed overnight with ice cold 70% ethanol while vortexing. The fixed cells were washed with PBS and stained with propidium iodide including, RNase A (1 mg/ml), and Triton X-100 (0.05% w/v) for 20 min in dark at 37 °C. Stained cells were quantified and fluorescence BD FACS Calibur™ flowcytometer for cell cycle with appropriate settings using CellQuest Pro software (BD).

Immuno-fluorescence microscopy

As previously performed in [26], cells were grown on glass coverslip inside a 6 well culture plate. Gedunin or inhibitor treated cells were washed with PBS, fixed using 4% formaldehyde in PBS (pH 7.3), permeabilized with 0.5% Triton X-100 for 10 min, washed and blocked with 2% BSA in TBST. Following this, the cells were washed, incubated with primary antibody (dilution 1:100) overnight at 4 °C, washed and incubated with Alexa-fluor conjugated secondary antibody (dilution 1:250) and Hoechst stain. Washed coverslips were inverted and mounted on glass slide with a drop of FluorSave™ Mounting media. Carl Zeiss LSM Meta 510 Confocal microscope with Plan Aplanachromat 63 \times oil/1.4 NA DIC objective lens was used for imaging with appropriate laser lines and excitation/emission filters.

Measurement of reactive oxygen species (ROS) levels

Intracellular level of ROS was determined using CM-H₂DCFDA, following manufacture's protocol from

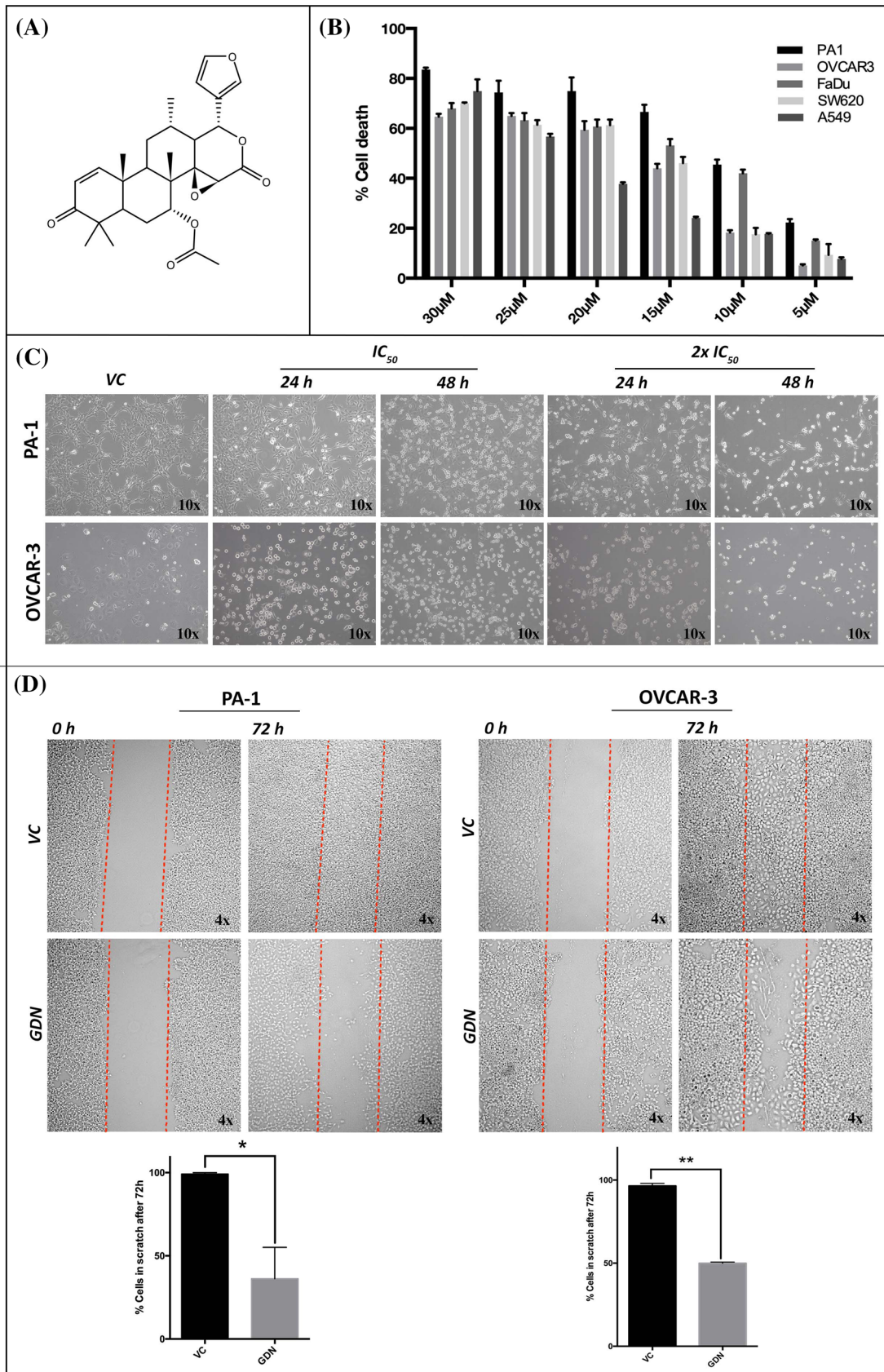


Fig. 1 Gedunin (GDN) inhibits proliferation of PA-1 and OVCAR—3 cells *in vitro*. **a** Chemical structure of Gedunin, **b** Cytotoxic effect of gedunin in human cancer cell lines at 48 h using SRB assay. **c** Phase contrast microscopy images of GDN treated PA-1 cells and OVCAR-3 cells at indicated dose and time points. **d** *in vitro* scratch healing assay in GDN treated PA-1 and OVCAR-3 cells as compared to untreated control cell at 72 h time point

Invitrogen (ThermoScientific). PA-1 or OVCAR-3 cells were grown to 50% confluence upon a glass cover slip, followed by treatment with gedunin for indicated time points, in presence of absence of ROS scavenger N-acetyl L-Cysteine (5 mM, co-incubated with gedunin). Post treatment, cells were then incubated with 10 μ M CM-H₂DCFDA for 30 min in dark, washed with PBS and examined live under confocal microscope (as mentioned in immuno-fluorescence section). Fluorescence intensity was measured using Zeiss LSM Image Examiner software.

Determination of mitochondrial membrane potential

Mitochondrial Membrane potential were measured using JC-1 dye as previously described in [27]. Gedunin treated cells were subjected to trypsin and washed with PBS. The cells were then incubated with JC-1 dye dissolved in incomplete media (20 μ M for 15 min at 37 °C in dark). Post washing in PBS, these were then immediately quantified with BD FACS Calibur flow cytometer at 488 nm using appropriate excitation/ emission filters and gating.

Phosphatidylserine exposure assay

Phosphatidylserine exposure assay was performed to quantify apoptotic population based on [28] as well as manufacturer's protocol described in BD Pharmingen™ Annexin FITC Apoptosis kit manual. Cells were cultured in 60 mm diameter tissue culture dishes up to 50% confluence and treated with gedunin or inhibitors for indicated time. Cells were harvested by trypsinization, washed twice with cold PBS and re-suspended in binding buffer (0.01 M HEPES, 0.14M NaCl, 2.5 mM CaCl₂ in aqueous solution, sterile). 10⁴ cells per sample re-suspended in 100 μ l binding buffer and were stained with FITC-conjugated Annexin V (as per manufacturer's protocol) and PI (2 μ g/ml) for 15 min at RT in dark. This was followed by adding 400 μ l of binding buffer and analysis in BD FACS Calibur flow-cytometer with appropriate controls and settings.

Western blotting

Gedunin treated cells at various time points were harvested and washed with cold PBS. The cell pellet was lysed for 1 h with cell lysis buffer (with protease and phosphatase

inhibitors) on ice, and whole cell protein was collected from the supernatant after centrifugation at 12,000 \times g at 4 °C. The protein samples were estimated using BCA protein estimation kit (as per manufacturer's protocol), and concentration-equalized samples were prepared using Lamelli's buffer (5 \times). Equal amount of protein were separated with SDS-PAGE, transferred onto PVDF membrane (0.45 μ m), blocked with 5% Bovine Serum Albumin/Nonfat dry milk, treated with primary antibody overnight (dilution 1:1000), and HRP conjugated secondary antibody (dilution 1:2500) for 2 h at room temperature, with intermittent washing between the steps with Tris buffered saline with Tween-20 (TBST). Blots were developed using Clarity ECL substrate using a Bio-Rad ChemiDoc XRS + system.

Scanning electron microscopy (SEM)

As previously reported from our lab in [27], PA-1 and OVCAR-3 cells were grown on glass cover slips, treated with gedunin and were fixed with 2.5% Glutaraldehyde (GA) in phosphate buffer (pH 7.3) overnight. After washing the cells were post fixed with 1% OsO₄ in phosphate buffer, washed and then dehydrated in ascending concentrations of ethanol. Cells were dried using a Critical Point Dryer and sputter coated with Au: Pd (80:20). The imaging was done using a FEI Quanta 250 Scanning Electron Microscope at 20 kV, using SE detector.

Transmission electron microscopy (TEM)

Cells for TEM analysis were prepared as reported earlier [29]. Briefly, gedunin treated cells were fixed with 2.5% Glutaraldehyde (GA) in phosphate buffer (pH 7.3). The fixed cells were washed and post fixed with 2% OsO₄ (in Phosphate buffer). Cells were dehydrated in ascending concentrations of ethanol followed by acetone, and finally embedded in Spurr resin. Ultra-thin sections (60–80 nm) sections were cut, picked on copper grids (200 mesh) and double stained with Lead citrate and Uranyl acetate. Imaging was performed with JEOL JEM 1400 Transmission Electron Microscope fitted with Gatan Orius SC200B CCD camera at 80 kV.

Statistical analysis

The statistical significance of the differences between two experimental groups from three independent experiments was assessed using two-tailed Student's t test. Differences were considered significant as P < 0.05 (*), < 0.01 (**), < 0.001 (***) and < 0.0001 (****). Software GraphPad-Prism™ was used for statistical analysis.

Results

Gedunin inhibits proliferation of ovarian cancer cells in vitro by inducing cell death

To investigate the anti-proliferative effect of gedunin, a panel of human cancer cell lines comprising pharyngeal cancer (FaDu), colon cancer (DLD-1), lung cancer (A549) and ovarian cancer (PA-1 and OVCAR-3) were treated with various concentrations of gedunin for 48 h, and results were quantified using sulforhodamine B (SRB) assay. Gedunin was found to inhibit the proliferation of all the cell lines in a dose dependent manner suggesting broad-spectrum inhibition in cancer types. As presented in Fig. 1b, ovarian cancer cell line PA-1 was found to be most susceptible to gedunin treatment with an IC_{50} value of 8.1 μ M. Therefore, further studies for mechanistic insights were performed in PA-1 cells. To substantiate our results in another ovarian cancer cell line OVCAR-3 cells were also selected for the mechanistic studies, for which the IC_{50} of gedunin was 18 μ M. Henceforth, the IC_{50} doses of PA-1 and OVCAR-3 cells have been used throughout this work. Moreover, IC_{50} values in FaDu, DLD-1 and A549 were determined to be 10.7 μ M, 14.8 μ M and 9.9 μ M respectively.

Phase contrast microscopy images (Fig. 1c) showed reduction in cell number and shrinkage in cytoplasmic volume in gedunin treated cells in a dose and time dependent manner indicating cell death in both PA-1 and OVCAR-3 cells respectively.

The in vitro scratch assay is a convenient assay to study cell migration in cultured cells [24]. Gedunin was found to inhibit migration in the scratch created in the monolayer when administered in IC_{50} doses for 72 h in PA-1 or OVCAR-3 cells as compared to complete healing of scratch in corresponding control cells (Fig. 1d). Therefore, these experiments indicate that gedunin inhibits proliferation and migration of ovarian cancer cells.

Gedunin causes G2/M phase arrest in ovarian cancer cells

Further, we examined the effect of gedunin on cell cycle progression of ovarian cancer cells using flow cytometry. PA-1 and OVCAR-3 cells were treated with gedunin at $0.5 \times IC_{50}$, IC_{50} and $2 \times IC_{50}$ for 12 h, 24 h and 48 h. Figure 2a, b show a significant increase ($p < 0.05$) in cell population at G2/M phase cell cycle arrest in both the cell lines at 24 and 48 h. Besides, as shown in PI intensity graphs in Fig. 2a, presence of a blue peak depicting Sub G_0 population or dead cells was observed after 24 h of gedunin treatment.

A G2/M phase arrest is an important checkpoint before a cell enters mitosis and ensures that genetic material has been meticulously duplicated before mitosis ensues [30]. Phosphatase cdc25 promotes cell division by binding to cyclin b and inhibition of cdc25 can lead to delay in cell cycle progression. Results in Fig. 2c show downregulation of cdc25 in both PA-1 and OVCAR-3 cell lines. Moreover, p21 (waf1/cip1) is a CDK inhibitor protein that suppresses cdk activity in event of DNA damage and thus cell cycle arrest [31]. The immunoblots results in Fig. 2c indicate a remarkable increase in p21 levels upon gedunin treatment in dose and time dependent manner, suggesting DNA damage could be responsible for cell cycle arrest. This was also corroborated by increase in phospho-p53 and phospho-H2A.X levels that indicate DNA damage [32, 33] (Fig. 4d).

Overall, results presented in Fig. 2 indicate that gedunin causes G2/M cell cycle arrest in a dose and time dependent manner by regulating cell cycle proteins in ovarian cancer cells which is followed by cell death.

Gedunin induces ultrastructural changes in ovarian cancer cells

Morphological and ultrastructural effects of gedunin in both PA-1 and OVCAR-3 cells were investigated using electron microscopy. SEM analysis (Fig. 3a, b) showed a decreased cell number characterized by reduced cell volume of PA-1 and OVCAR-3 cells. Rounding up of cells with blebbings and apoptotic bodies were observed in gedunin treated cells. The cells were noticeably reduced in size (Fig. 3a(ii–iii), b(ii–iii)), as compared to flat, polygonal epithelial morphology of vehicle control cells (Fig. 3a(i), b(ii)).

Subcellular changes in gedunin treated cells were observed under TEM. Decreased cytoplasmic content with cell shrinkage, pyknosis and nuclear fragmentation but intact plasma membrane (Fig. 3c(ii–iv), d(ii–iv)) were noticed in treated cells. In contrast, the control cells were elongated with intact double membrane bound nucleus, and with normal ultrastructure of the organelles (Fig. 3a(i), b(i)). Late stage effects of (upto 48 h) gedunin included severe vacuolation with appearance of multi-lamellar bodies (Fig. 3c(iv) and d(iii) and (iv)). Mitochondria in treated cells were observed to be remarkably affected suggesting mitochondrial stress characterized by acute swelling and disrupted cristae (Fig. 3c(vi–vii), d(vi–vii)) as compared to mitochondrial ultrastructure in control cells (3C(v) and 3D(v)) with intact cristae and overall normal morphology. Endoplasmic reticulum (ER) stress was not observed in both gedunin treated PA-1 and OVCAR-3 cells (Fig. 3c(viii), d(viii)). The ultrastructural changes were attributed to hallmark morphological

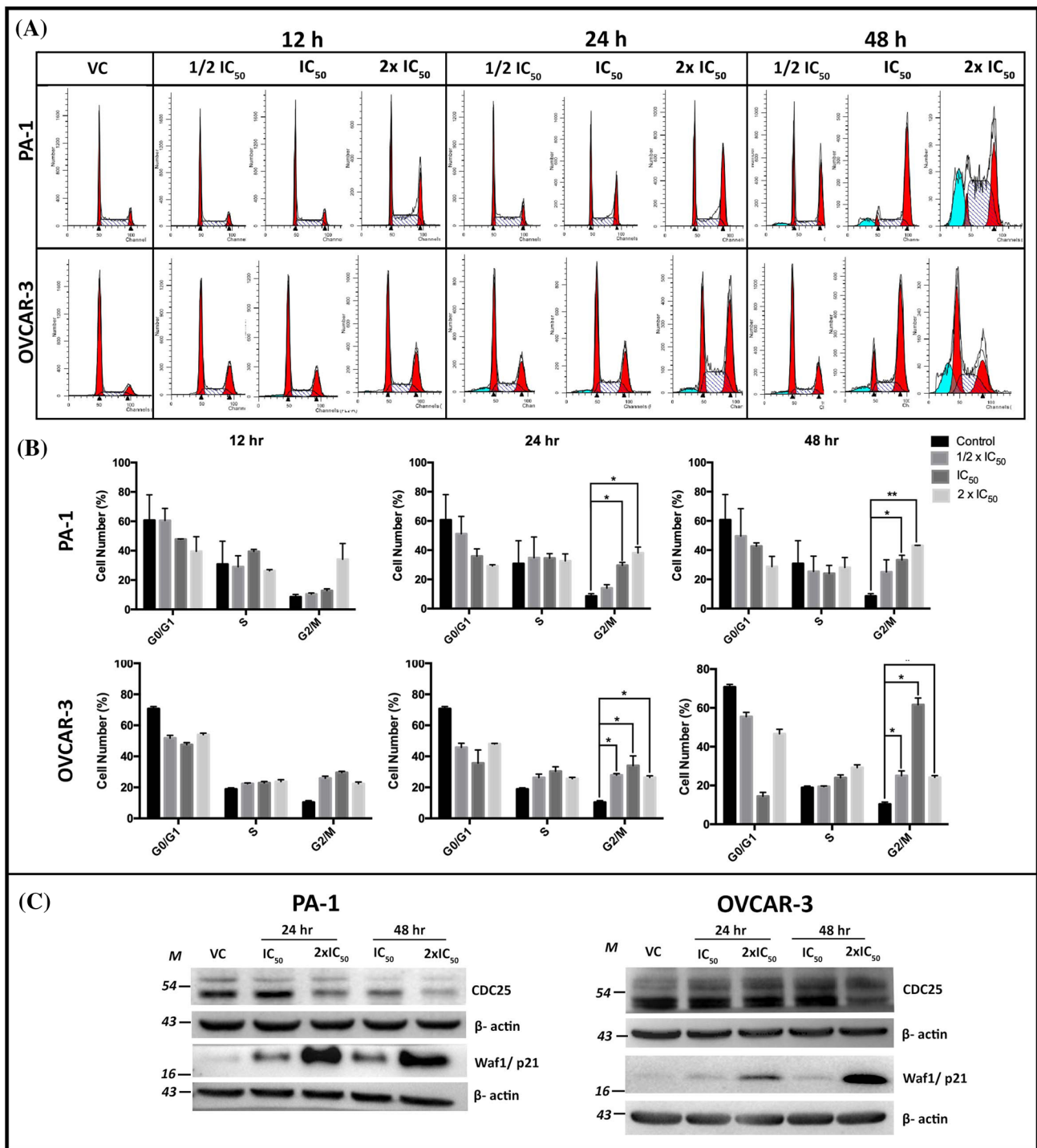


Fig. 2 Gedunin causes G2/M phase arrest in ovarian cancer cells. **a** Flow Cytometry analysis based propidium iodide (PI) intensity plot of GDN treated PA-1 and OVCAR-3 cells at indicated dose and time point showing shift towards G2/M peak with dose and time. **b** The

quantified bar graph of cell population in each cell cycle phase as indicated dose and time points. (p value * < 0.05, ** < 0.01). **c** Western blot of cell cycle proteins in ovarian cancer cells following GDN treatment at indicated dose and time points

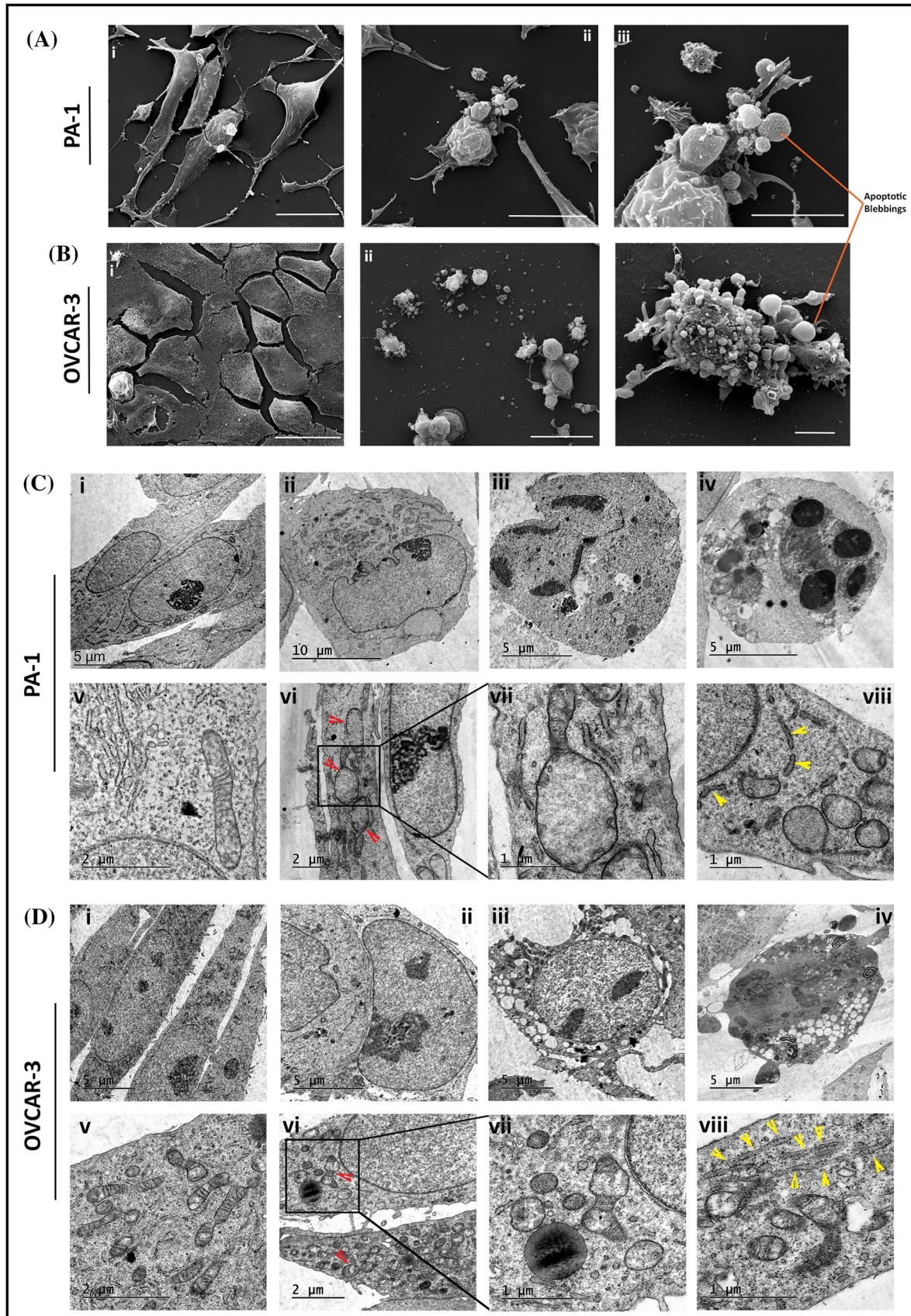


Fig. 3 Representative electron micrographs revealing the morphological effects of gedunin. **a** and **b** represent SEM micrographs showing topological changes observed in PA-1 or OVCAR-3 cells respectively following GDN treatment, where **a**(iii) and **b**(iii) represent magnified images of apoptotic cells. Blebs/Apoptotic bodies can be seen emanating off the cell(s) undergoing apoptosis. (Scale bar = 10 μ m in **a**(i–ii) and **b**(i–ii), and 5 μ m in **a**(iii) and **b**(iii)). **c** and **d** Representative transmission electron micrographs showing early to late apoptotic features in PA-1 cells **c**(ii–iv) as compared to control cells in **c**(i); and in OVCAR-3 cells **d**(ii–iv) as compared to control cell in **d**(i). Micrographs in **c**(vi–vii) and **d**(vi–vii) represent effect of GDN on mitochondria which are observed to be swollen with disrupted cristae (red arrows) of PA-1 and OVCAR-3 cells as compared to their normal morphology in **c**(v) or **d**(v) respectively. **c**(viii) and **d**(viii) represent endoplasmic reticulum (ER) (indicated by yellow arrows) in GDN treated PA-1 and OVCAR3 cells respectively (Color figure online)

features of apoptosis, which was in agreement with our biochemical findings. Together, these results show that gedunin induces detrimental ultrastructural changes in ovarian cancer cells suggestive of apoptotic cell death.

Gedunin causes mitochondrial depolarisation and promotes apoptosis in ovarian cancer cells

Taking cues from our TEM observations, we further explored the physiological effects of gedunin in PA-1 and OVCAR-3 cells. A steady mitochondrial membrane potential (MMP) is important for normally functioning mitochondria in healthy cells, which is depolarized under stress conditions [34]. JC-1 is a cationic dye that form J-aggregates with intense red fluorescence in healthy mitochondria and is dispersed in monomeric green fluorescent form in depolarized mitochondria. As shown in Fig. 4a, gedunin treated cells showed significant ($p < 0.01$) mitochondrial depolarization in a dose dependent manner, confirming mitochondrial stress. Carbonyl cyanide *m*-chlorophenyl hydrazine (CCCP) was used as positive control, which is a mitochondrion depolarizing agent, where more than 90% of the cells had depolarized MMP.

To confirm the nature of cell death, we performed phosphatidylserine exposure assay to differentiate between early/late apoptotic and necrotic cell populations. Two to five-fold increase in apoptotic quadrants (Annexin⁺/PI⁻ and Annexin⁺/PI⁺) were observed in gedunin exposed cells indicating apoptosis (doxorubicin was used a positive control) (Fig. 4b). This result was in agreement with our ultrastructural findings that presented classical structural features of apoptosis in gedunin treated cells (Fig. 3).

Apoptotic mode of cell death normally occurs via the intrinsic or extrinsic pathways, which are mediated by different sets of molecular machineries. Results in Fig. 4c, d confirm that gedunin induces apoptosis via intrinsic pathway which involves mitochondria. The release of cytochrome c from the mitochondrial intermembrane space is a decisive

feature in apoptosis and is generally considered as ‘point of no return’ [35]. We performed immunofluorescence staining to observe the distribution pattern of cytochrome c using confocal microscopy. As presented in Fig. 4c, control cells showed a mitochondrial pattern of cytochrome c (green fluorescence), but in gedunin treated cells it had clearly translocated to the cytoplasm from the mitochondria following gedunin treatment indicating onset of apoptosis. Pre-treatment of PA-1 cells with pan-caspase inhibitor z-VAD-fmk following gedunin treatment resulted in mitochondrial localization of cytochrome c similar to control cells, suggesting inhibition of caspase dependent apoptosis.

Western blot data in Fig. 4d from gedunin treated PA-1 and OVCAR-3 cells also supported these findings as phospho-H2A.X and phospho p53 levels were found to be increased. Furthermore, following cytochrome c release, Caspase 9 is activated and leads to activation of caspase 3—an executioner caspase and leads to proteolytic cleavage of many key proteins including poly (ADP) ribose polymerase (PARP), whose cleavage facilitates cellular disassembly leading to cell death. Bax also contributes to apoptosis by translocation to mitochondria and facilitating cytochrome c release [36], while Bcl2 plays anti-apoptotic role by inhibiting cytochrome c release and caspase activity. The overall Bax/Bcl2 ratio was found increased in gedunin treated cells as compared to control cells, with increasing dose and time points, indicating progression of apoptosis. Our results show increased expression of Bax, cyt c release, activation of caspase 9 and caspase 3, and PARP cleavage in dose and time dependent manner. These observations confirmed caspase dependent mitochondrial apoptosis by gedunin in ovarian cancer cells.

Gedunin triggers ROS generation in ovarian cancer cells

Reactive oxygen species (ROS) are by-products of metabolism inside the cells, generated inside mitochondria by the electron transport chain, and are maintained at a low concentration by the intrinsic cellular antioxidant system. Excessive ROS generation has been linked to DNA damage, intracellular stress, and contributes to cell death. Our earlier observations of mitochondrial stress and damage prompted us to evaluate the ROS levels in gedunin treated cells using fluorogenic probe CM-H₂DCFDA at various time points. Confocal microscopy results in Fig. 5a indicate significant up-regulation ($p < 0.0001$ in PA-1 and $p < 0.001$ in OVCAR-3) of cytoplasmic ROS levels in PA-1 and OVCAR-3 cells, treated with corresponding IC₅₀ doses of gedunin, from 3 h time point onwards indicating ROS production to be an early event following gedunin treatment. ROS production

Fig. 4 Gedunin causes mitochondrial depolarization and induces apoptosis. **a** Mitochondrial membrane potential measurement using JC-1 dye in PA-1 and OVCAR-3 at mentioned dose points and quantified bar graph in **a(ii)** (P value * < 0.05, ** < 0.01). **b** Phosphatidylserine exposure assay in PA-1 to evaluate percentage of cells in early or late apoptosis at indicated time points and in presence of Doxorubicin (Positive control). **c** Immunofluorescence experiments using confocal microscopy showing translocation cytochrome c in GDN treated cell (in green channel 488 nm) in PA-1 cells compared to control cells and GDN treatment in presence of pan caspase inhibitor z-VAD-fmk (co-treated, 20 μ m). **d** Western blot analysis of DNA damage and apoptosis markers in PA-1 and OVCAR-3 cells (Color figure online)

was found significantly quenched ($p < 0.001$) in presence of antioxidant N-acetyl L cysteine (NAC) (Fig. 5b).

Further, we stained the gedunin treated PA-1 cells with MitoSOX Red, a dye that is specifically selective for superoxide species in the mitochondria. The results in Fig. 5c show dose dependent increase in mitochondrial superoxide levels, which was found to be significantly ($p < 0.0001$) quenched in presence of antioxidant NAC, thus suggestive of production of superoxide species in gedunin treated cells.

Oxidative stress contributes to G2/M phase cell cycle arrest and mitochondrial depolarisation

Previous results have demonstrated ROS generation, DNA damage, G2/M cell cycle arrest and mitochondrial depolarisation following gedunin treatment in PA-1 and OVCAR-3 cells. This prompted us to explore the role of ROS in mediating cell cycle arrest and mitochondrial dysfunction. We performed cell cycle analysis (using flow cytometry) of gedunin treated PA-1 cells in presence of ROS quencher NAC. Results in Fig. 5d, presents the graphs of PA-1 and OVCAR-3 cell population in various phases of cell cycle in presence or absence of NAC following gedunin treatment. Our results demonstrate that there was a significant ($p < 0.05$) reduction in G2/M population in both PA-1 and OVCAR-3 cell when the cells were co-treated with NAC to quench cellular ROS, while only gedunin treated cells were found stalled in G2/M phase.

We also investigated whether or not NAC could restore the MMP loss observed earlier with gedunin treatment. Our results in Fig. 5d present that mitochondrial depolarization was averted in presence of NAC. A decreased number of cells with depolarized MMP were observed (from 54.2 to 33.8% in PA-1 cells and from 34.7 to 24.5% in OVCAR-3 cells) in presence gedunin alone or with NAC treatment respectively. These results therefore indicate that ROS generation by gedunin is upstream of cell cycle arrest and mitochondrial membrane depolarization, and that presence of ROS quencher NAC could rescue cells from these effects.

Gedunin treatment leads to activation of MAP kinases and inhibition of proliferation signalling pathways

Mitogen activated protein kinases (MAP kinases) are sequentially activated protein kinases that play vital role in signal transduction and can be categorized into extracellular regulated kinases (ERK), c-Jun N terminal Kinase (JNK) and Stress activated protein kinases (SAPK/p38 MAPK), where JNK and p38 MAPK play important roles during inflammation, environmental stress and apoptosis [37].

Immunoblot results in Fig. 6A show increased expression MAP kinases including phospho p42/44 MAPK (ERK), phospho JNK and phospho p38 suggesting a wide response to intra-cellular stress, in a dose and time dependent manner following gedunin treatment in PA-1 cells. A prolonged activation of JNK has been linked to suppression of inactivators of mitochondrial-mediated apoptosis [38]. Thus, our results indicate that MAP kinase activation by gedunin is a key component of its response towards apoptotic pathway.

We also evaluated the expression of ER stress markers like GRP78 and CHOP/GADD153 that contribute to unfolded protein response. However, as seen in immunoblots shown in Fig. 6b, there was no significant increase in expression of these markers. This observation is supported by our TEM results that showed no luminal swelling in ER in gedunin treated PA-1 or OVCAR-3 cells. Furthermore, a decreased expression of proliferative pathways markers like phospho-mTOR (Ser2448), JAK2 and STAT3 in gedunin treated PA-1 cells was observed in immunoblots (Fig. 6b). As these proteins are clients of HSP90 complex, these results support the previous observations that gedunin inhibits cell proliferation in ovarian cancer cells[39].

Further, we sought to evaluate if activation of MAP kinase (phospho p42/44) was related to ROS generation. Gedunin treated cells were subjected to U0126 treatment (phospho p42/44 MAPK inhibitor), and then followed by gedunin treatment. ROS level were measured in these cells using CM-H2DCFDA (Fig. 6c). There was no significant decrease in ROS levels with U0126 in gedunin treated cells, however, phospho p42/44 MAPK levels were found to be decreased in presence of NAC, indicating that ROS generation event is probably upstream of MAP Kinase activation (Fig. 7a).

ROS generation and Stress kinases contribute to gedunin induced apoptosis in ovarian cancer cells

To further dissect the role of ROS in promoting apoptosis, we administered gedunin treated cells with inhibitors like NAC (antioxidant), z-VAD-fmk (pan-caspase inhibitor) and evaluated the markers for DNA damage, cell cycle arrest in G2/M phase, stress kinases and apoptosis (Fig. 7).

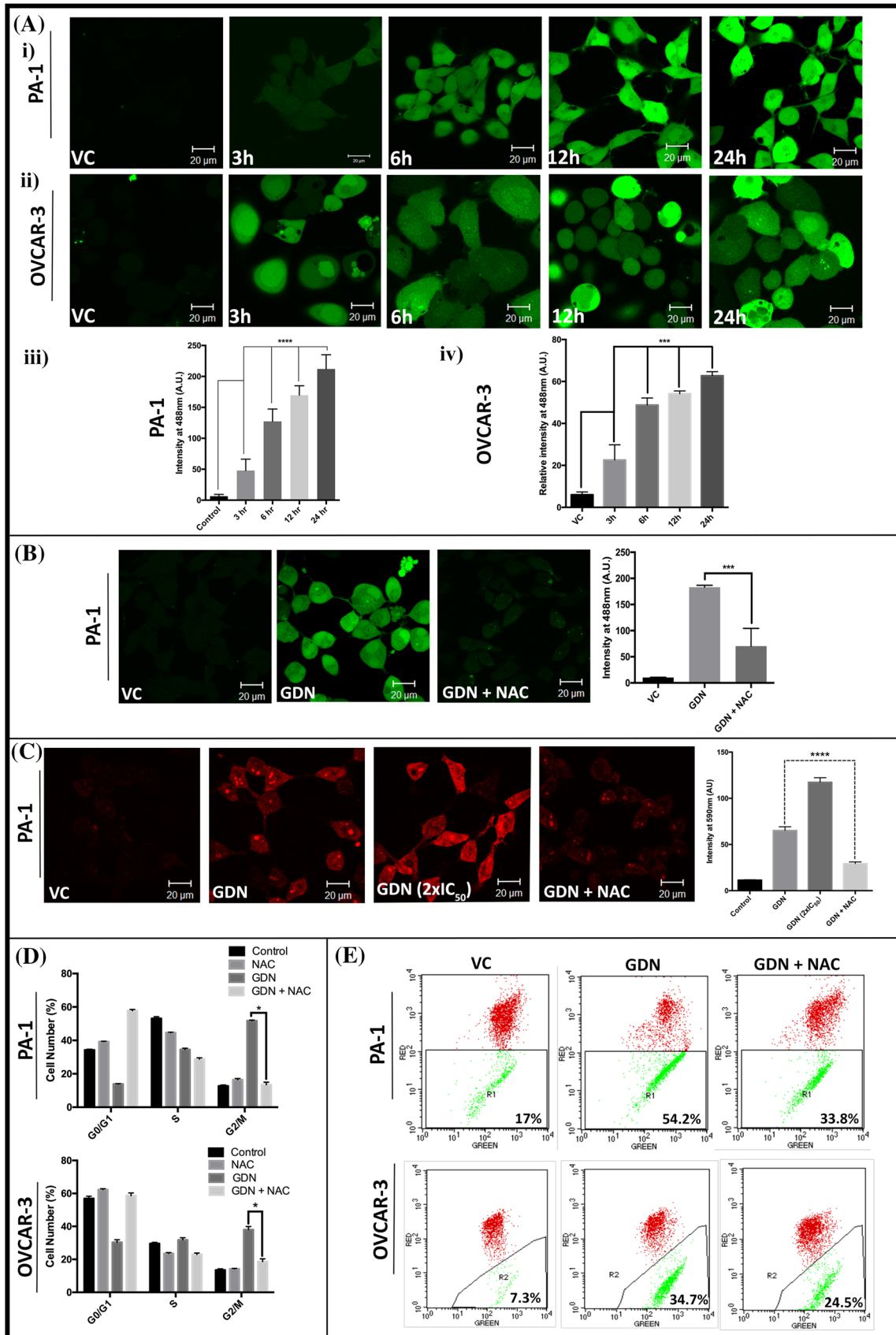


Fig. 5 Gedunin triggers ROS generation in ovarian cancer cells leading to cell cycle arrest and mitochondrial membrane depolarization. **a**(i) and (ii) represent confocal micrographs of CM-H₂DCFDA stained PA-1 or OVCAR-3 cell treated with IC₅₀ dose of GDN at indicated time points and corresponding intensity plots in (iii) for PA-1 and (iv) for OVCAR-3 as measured for 50 cells from each time point. **b** ROS levels in presence of antioxidant NAC at 5 mM (for PA-1) or 3 mM (for OVCAR-3) co-treatment with IC₅₀ doses of GDN for PA-1 and OVCAR-3 cells respectively for 24 h. **c** Confocal micrographs representing fluorescence of Superoxide levels using MitoSox dye in PA-1 cells at indicated dose of GDN for 24 h, in presence of NAC. Quantified bar graph of fluorescence intensity (for 50 cells); indicating super oxide generation in PA-1 cells upon GDN treatment. **d** Bar graph of cell cycle analysis of IC₅₀GDN treated (48 h) PA-1 and OVCAR-3 cells in presence of NAC indicating decrease in G2/M phase cells. **e** Mitochondrial membrane potential (analyzed using JC-1 dye staining in flowcytometer) in PA-1 and OVCAR-3 cell following GDN treatment IC₅₀ (24 h) in presence of NAC. (p value corresponds to * < 0.05, ** < 0.01, *** < 0.0001)

As presented in Fig. 7a, the immunoblotting results show expression of indicated proteins in gedunin treated cells with NAC co-incubation compared with only gedunin treatment. It was observed that NAC was able to reverse almost all of the detrimental effects of gedunin induced cellular insults. DNA damage markers phospho H2A.X, phospho p53 and p21 were found be downregulated in presence of NAC. We had observed that gedunin treatment results in decreased expression of CDC25C (Fig. 5c). Interestingly, NAC treatment restored CDC25 level indicating abrogation of cell cycle arrest. A decrease in phospho JNK and phospho p42/22 MAPK was also observed in presence of NAC, confirming our observations in Fig. 6c. Finally, apoptotic markers like caspase 3 and PARP cleavage were also found to be decreased in presence of NAC indicating that ROS triggered apoptosis in PA-1 cells.

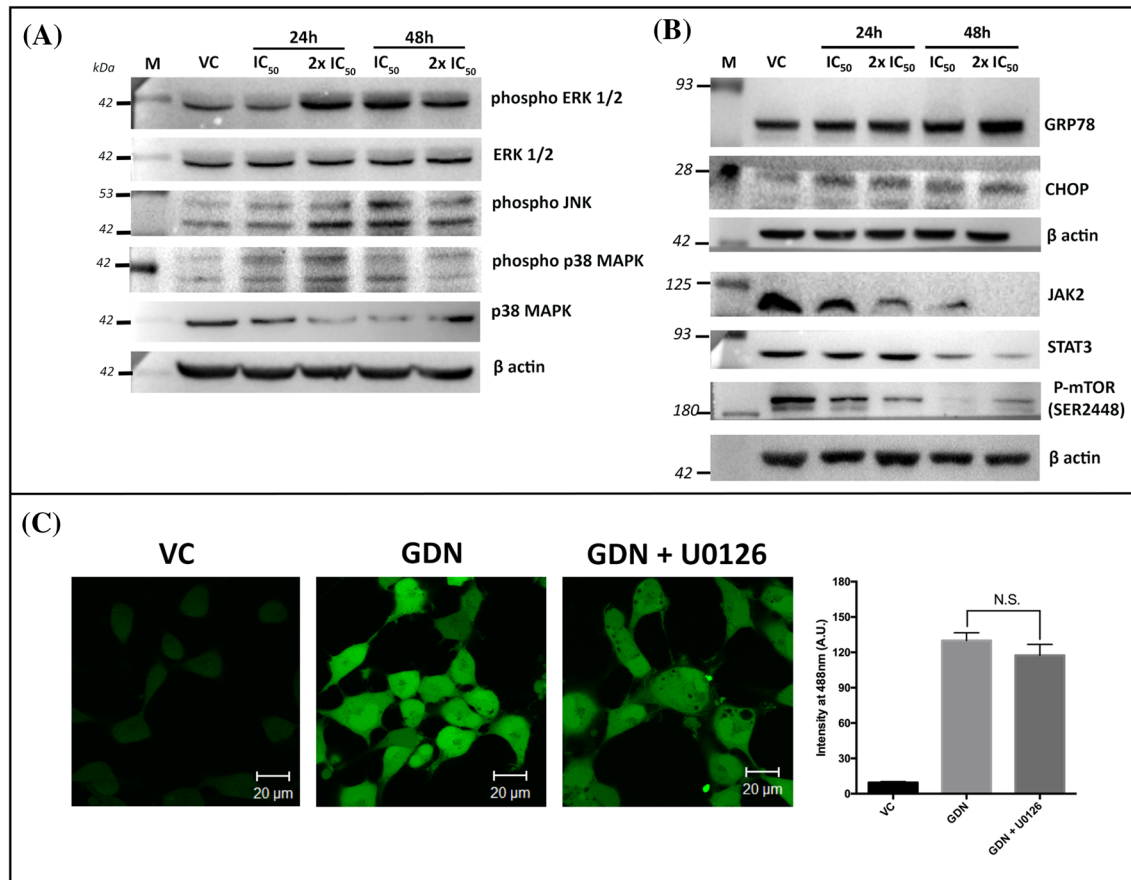


Fig. 6 Gedunin leads to activation of MAP kinases and inhibition of proliferative pathways. **a** Immunoblots showing MAP kinases upregulation in GDN treated PA-1 and indicated dose and time points. **b** Immunoblots of GDN treated PA-1 cells showing expression levels of ER stress markers: GRP78 and CHOP, as well as of proliferative pathways JAK-STAT and phospho-mTOR (Ser 2448). **c** Confocal

micrographs of DCFDA intensity for ROS levels PA-1 cells in presence of U0126 (phospho-ERK inhibitor) (pre-treatment 2 h, 20 μm, incomplete media) and Intensity bar graph of confocal micrographs of ROS levels in presence of ERK inhibitor U0126 and IC₅₀ dose of GDN for 24 h showing no significant decrease in level of ROS in presence of U0126

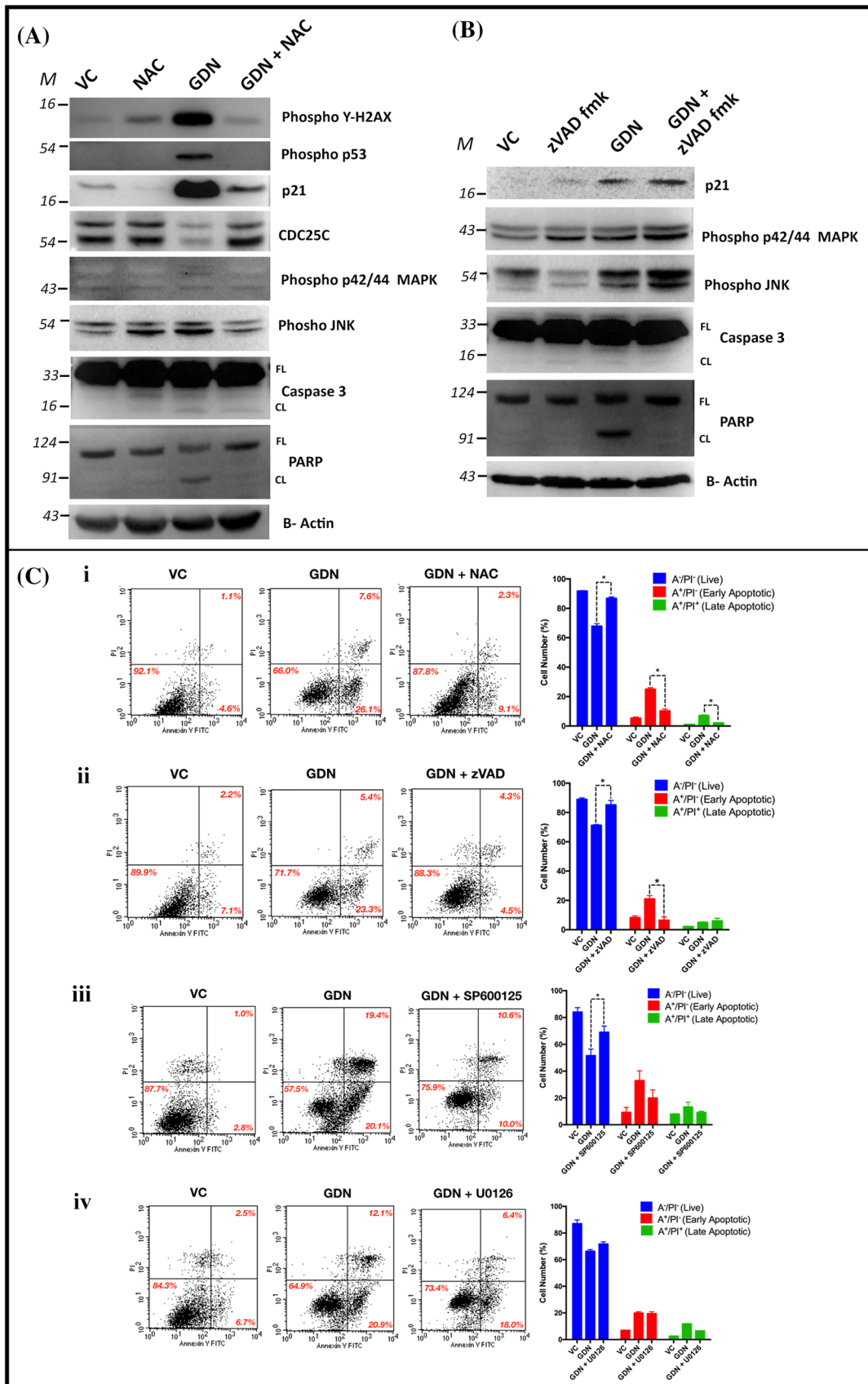


Fig. 7 ROS and Stress kinases contribute to gedunin induced apoptosis in ovarian cancer cells. Immunoblot analysis of DNA damage, cell cycle, and apoptosis markers in PA-1 cells in presence of **a** ROS quencher NAC (5 mM co-treatment) and, **b** Pan caspase inhibitor z-VAD-fmk (20 μ m co-treatment) with IC_{50} dose of GDN. **c**(i) to (iv) shows cell viability measured using phosphatidylserine exposure assay in gedunin treated PA-1 cells in presence of (i) NAC (ii) z-VAD-fmk (iii) SP600125 and (iv) U0126

Similarly, we tested the effects on the aforementioned markers following gedunin treatment with or without z-VAD-fmk (pan-caspase inhibitor) as shown in Fig. 7b. We observed that gedunin treatment in presence of z-VAD-fmk had no effect on p21, phospho p42/44 MAPK and phospho JNK levels; while a decrease in expression profile of caspase 3 and PARP cleavage was observed.

Inhibition of ROS generation, MAPK activation and Caspase activation effects cell viability in gedunin treated ovarian cancer cells

Using flow cytometry, we also performed phosphatidylserine exposure assay (by Annexin/PI staining) to study the effect on cell viability of PA-1 cells in presence of gedunin with or without NAC (ROS inhibitor), z-VAD-fmk (caspase inhibitor), U0126 (phospho ERK inhibitor) or SP600125 (JNK inhibitor). As presented in Fig. 7c(i) there was significant increase ($p < 0.05$) in healthy cell population (Annexin⁻/PI⁻), and significant decrease ($p < 0.05$) in both early and late apoptotic cell (Annexin⁺) population in presence of NAC in gedunin treated cells. Therefore, this result confirms gedunin induced oxidative stress is an upstream event and its inhibition using ROS quencher NAC can rescue of cells from undergoing apoptosis. In presence of pan caspase inhibitor z-VAD-fmk (Fig. 7ciii) in gedunin treated cells, a significant ($p < 0.05$) increase in population of live cells and a significant ($p < 0.05$) decrease in population of early apoptotic population was observed as compared to live and early apoptotic population in vehicle control. However, z-VAD-fmk could not rescue late apoptotic cells (p value not significant) as compared to late apoptotic population in only gedunin treated cells.

Moreover, as MAP kinases activation was observed in our previous results (Fig. 6a), we further studied effects of MAP kinase inhibition on cell viability of gedunin treated cell, using pharmacological inhibitors of JNK (SP600125) and phospho ERK (U0126). As shown in Fig. 7c(iii), we observed a significant ($p < 0.05$) rescue of cells upon gedunin treatment with SP600125, and a decrease in early apoptotic population was also observed. Furthermore, as presented in Fig. 7c(iv) there was no significant rescue of cells nor decrease in apoptotic population in gedunin treated cell in presence of U0126. These observations collectively suggest that caspase mediated apoptosis induced by gedunin

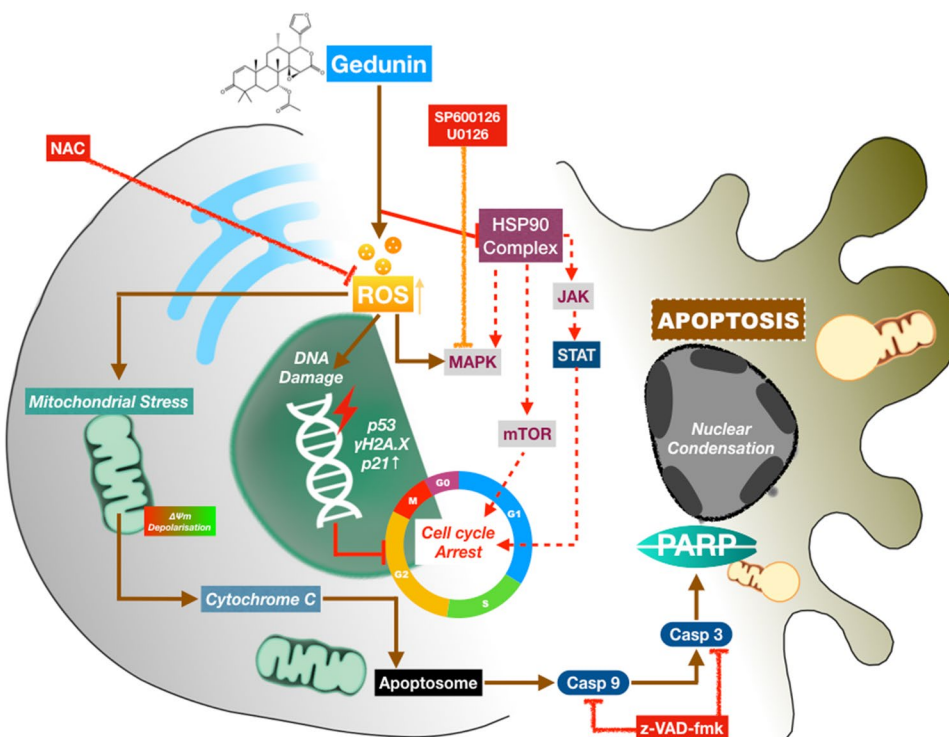
is initiated by ROS upregulation and is mediated by JNK, while ERK alone may not have a role in apoptosis induced by gedunin.

Discussion

Cancer cells are generally characterized by dysregulated ROS levels, uncontrolled proliferation and altered physiology. Although, modulation of oxidative stress has been implicated to provide a source of mutation to cancer cells for survival in hostile environments, but a growing number of evidences also suggest an abnormal increase in ROS can also be exploited to induce cell death of cancer cells [40]. Here, we have demonstrated that the tertranortriterpenoid gedunin, inhibits the growth of ovarian cancer cells in vitro through induction of severe oxidative stress, cell cycle arrest and mitochondrial mediated apoptosis (Fig. 8). Interestingly, gedunin has previously been reported to inhibit the HSP90 complex machinery which is central in driving carcinogenesis by chaperoning client oncogenic proteins [41]. Inhibiting cell proliferation is a crucial step in managing cancer cell growth. In accordance with previous reports, our results confirm gedunin has inhibitory effect on multiple origin cancer cells including ovarian teratocarcinoma (PA-1) and adenocarcinoma (OVCAR-3) origin cells. Significant inability of cells to grow back in the scratch assay also supported the potency of gedunin to inhibit cell proliferation. Furthermore, the G2/M phase is an important checkpoint which ascertains that genetic material is intact and the cells' division machinery is fully prepared. This is regulated by CDC25, a dual specificity phosphatase that promotes de-phosphorylation of cyclin B complex for entry into mitosis. Since CDC25C is itself an HSP90 client [39], therefore its downregulation is likely due to gedunin's HSP90 inhibition. Moreover, p21 is also a regulator of cell cycle and apoptosis following DNA damage and is regulated by both p53 dependent and p53 independent mechanisms [42]. An increase in p21 was also observed in gedunin treated cells indicating its role in cell cycle arrest.

Gedunin was also found to activate MAP kinases SAPK/JNK and p44/42 MAPK (also called ERK). Similar mechanisms of action have been widely reported for natural [43–45] and synthetic [46, 47] compounds with some important differences. Firstly, JNK activation usually activates autophagy pathway by inhibiting phosphorylation of mammalian target of rapamycin (mTOR) and thus activation of autophagy kinase ULK1 (Unc-51 like autophagy activating kinase1) [48]. Although we found p-mTOR to be downregulated, this did not result in autophagic activity as measured through LC3 lipidation (data not shown) and TEM analysis. This suggests that the downstream target of mTOR inhibition in this case could be non-autophagic factors primarily

Fig. 8 Schematic representation of proposed mechanism of action of Gedunin in ovarian cancer cells



associated with cell cycle regulation, such as 4EBP1 and S6 kinase [49]. Second, the activation of another MAPK family member, ERK is surprising. ERK activation usually proceeds through mitogen and growth factor signaling and leads to cell proliferation, and also toward the epithelial-to-mesenchymal transition (EMT) in cancer cells [50]. ERK activation with GDN treatment can be speculated as a stress response mechanism to drive proliferation of cancer cells against free radical stress. Indeed, mitochondrial ROS have been shown earlier to activate ERK as a stress response mechanism in prostate cancer cells [51]. Notably, as found in cell viability analysis using JNK and ERK inhibitors in presence of gedunin (Fig. 7ciii and iv), pharmacological ERK inhibition did not confer a survival benefit to gedunin treatment of ovarian cancer cells; as opposed to JNK inhibition where an increased viability of cells was observed. This implies that probably JNK has a more significant role than ERK in contributing to ovarian cancer cell death upon gedunin treatment.

ROS is a long-standing mediator of apoptotic cell death which opens the mitochondrial permeability transition pore (MPTP) leading to release of cyto-c and AIF (apoptosis inducing factor) from mitochondrial intermembrane space. Cyt-c and AIF drive subsequent activation of Apaf-1 (apoptotic protease activating factor-1). Apaf-1 oligomerizes together with caspase-9 (an initiator caspase) to form apoptosomes, which act downstream on executioner caspases like caspase-3 and 7 to switch on the intrinsic program [52]. The activation of JNK is also tied very closely with ROS/RNS

generation and apoptosis, since upstream kinases ASK1 (a MAPKKK) and Src are reported to be directly activated by ROS species like H_2O_2 , and follow the downstream cascade leading to JNK activation [53]. Here, we see that inhibiting JNK by SP600125 led to rescue of increased viability of gedunin treated cells, in a manner similar as the ROS quencher, NAC. This can mean that majority of the ROS signaling proceeds through JNK activation for an apoptotic fate. Moreover, it is well-known that JNK is responsible for ROS production in the mitochondria (especially mitochondrial superoxides) after activation and subsequent mitochondrial translocation [54]. This can explain the increased MitoSOX signal in GDN-treatment which was reduced with NAC. Moreover, activated JNK also modifies the function of pro- and anti-apoptotic members of the Bcl-2 family like Bax, Bim and Bcl-2 to activate apoptosis [55], which is also in line with our observations.

Cancer cells deploy a multitude of survival strategies for evasion of immune response and stressful conditions like nutrient scarcity, hypoxia, proteotoxic stress, leading to serious malignancies. HSP90 complex is one central molecular machinery that helps cancer cells to survive proteotoxic stress [41, 56]. While most HSP90 inhibitors (like 17-AAG and tanespimycin) tend to block the ATP binding pocket with HSP N-terminal ATP binding pocket as well as induce over expression of anti-apoptotic HSP70 and HSP27 co-chaperones that reduces the HSP90 activity, gedunin has been shown to bind to p23 co-chaperone of the HSP90 complex [10] and not directly compete for the

ATP binding pocket of the HSP90. Our results also stand in concordance with mechanisms of other HSP90 inhibitors like NUP-AUY922 and Ganetispib which have been reported in glioblastoma and pancreatic cancer respectively [57, 58], and cause G2/M cell cycle arrest, MAPK activation and inhibition of proliferative pathways. However, a severe oxidative stress and mitochondrial stress as principal reasons for cell death seems more exclusive to gedunin as compared to other HSP90 inhibitors. Terpenoids isolated from natural sources like celastrol and wentilactone have been shown to have inhibitory effects on various cancer types including pancreatic cancer, breast cancer, and have been found to have lesser toxicity in non-cancer cells [59, 60]. Gedunin and celastrol are among same class of compounds chemically and both are HSP90 inhibitors. However, a major difference between both the molecules was that celastrol also induces autophagy in cancer cells leading to apoptosis, while gedunin was not found to induce autophagy in ovarian cancer cells. These molecules have been found to induce ROS, G2/M cell cycle arrest, modulate signalling lead to intrinsic apoptosis, highlighting gedunin's mechanistic similarity to other terpenoids.

Moreover, *Xylocarpus granatum* (Mangrove cedar) and *Azadirachta Indica* (neem) which are rich sources of gedunin have been in use for a long time in traditional medicine as anti-diarrheal, anti-malarial, anti-filarial and traditional anti-diabetic [10, 13, 18, 61] and highlight the potency of natural terpenoids for prospective drug development.

Finally, given that ovarian cancer is on rise worldwide, and contributes significantly to morbidity and mortality among women, there is a need for newer, safer and strategic therapies to further improve therapeutic outcomes in patients. While the present study was conceived to explore the in vitro mechanistic basis of the anti-proliferative action of gedunin, future in vivo studies assessing the findings in ovarian tumor models will be required in order to establish it as a viable anti-ovarian cancer treatment option.

Acknowledgements Technical assistance from Ms. Garima Pant and Mrs. Madhuli Srivastava for EM specimen preparation at EM Unit SAIF-R CDRI; and Mr. AL Vishwakarma and Mrs. Madhu Chaturvedi for flow-cytometer analysis, SAIF-R CDRI is acknowledged. This is CDRI communication number 10065.

Author contributions RS performed most of the experiments, prepared figures and wrote the first draft of the manuscript; AB performed some experiments and edited manuscript; VNS, PY, TN isolated gedunin; JS provided critical inputs and shared resources; MH performed cell viability assay supervised by JS; TN and KM conceived the study; KM supervised the study, interpreted data, arranged funding, edited and finalized the manuscript.

Funding Funding support from CSIR network project BSC0120 and institutional project OLP0101 to KM, fellowship DBT-SRF to RS, CSIR-SRF to AB, CSIR-SRF to PY and ICMR-SRF to MH is duly acknowledged.

Compliance with ethical standards

Conflict of interest The authors declare that there are no conflicts of interest.

References

1. Reid BM, Permuth JB, Sellers TA (2017) Epidemiology of ovarian cancer: a review. *Cancer Biol Med* 14:9–32. <https://doi.org/10.20892/j.issn.2095-3941.2016.0084>
2. Maheshwari A, Kumar N, Mahantshetty U (2016) Gynecological cancers: a summary of published Indian data. *South Asian J Cancer* 5(3):112–120. <https://doi.org/10.4103/2278-330X.187574>
3. <https://www.cdc.gov/cancer/ovarian/statistics>
4. <https://seer.cancer.gov>. Cancer Stat Facts: Ovarian Cancer. NIH National Cancer Institute
5. Li SS, Ma J, Wong AST (2018) Chemoresistance in ovarian cancer: exploiting cancer stem cell metabolism. *J Gynecol Oncol* 29(2):1–11. <https://doi.org/10.3802/jgo.2018.29.e32>
6. Mileo AM, Miccadei S (2016) Polyphenols as modulator of oxidative stress in cancer disease: new therapeutic strategies. *Oxid Med Cell Longev* 2016(1):17
7. Hasanain M, Bhattacharjee A, Pandey P et al (2015) α -Solaniene induces ROS-mediated autophagy through activation of endoplasmic reticulum stress and inhibition of Akt/mTOR pathway. *Cell Death Dis* 6(8):e1860–e1814. <https://doi.org/10.1038/cddis.2015.219>
8. Yao W, Lin Z, Shi P, Chen B, Wang G, Huang J (2020) Delica flavone induces ROS-mediated apoptosis and inhibits PI3K/AKT/mTOR and Ras/MEK/Erk signaling pathways in colorectal cancer cells. *Biochem Pharmacol* 171(October 2019):113680. <https://doi.org/10.1016/j.bcp.2019.113680>
9. Kuttan G, Pratheeshkumar P, Manu KA et al (2011) Inhibition of tumor progression by naturally occurring terpenoids Inhibition of tumor progression by naturally occurring terpenoids. *Pharm Biol* 49(10):995–1007. <https://doi.org/10.3109/13880209.2011.559476>
10. Patwardhan CA, Fauq A, Peterson LB, Miller C, Blagg BSJ, Chadli A (2013) Gedunin inactivates the co-chaperone p23 protein causing cancer cell death by apoptosis. *J Biol Chem* 288(10):7313–7325. <https://doi.org/10.1074/jbc.M112.427328>
11. Uddin SJ, Nahar L, Shilpi JA et al (2007) Gedunin, a limonoid from *xylocarpus granatum*, inhibits the growth of CaCo-2 colon cancer cell line in vitro. *Phyther Res* 761(21):757–761. <https://doi.org/10.1002/ptr>
12. Brandt GEL, Schmidt MD, Prisinzano TE, Blagg BSJ (2008) Gedunin, a novel hsp90 inhibitor: semisynthesis of derivatives and preliminary structure–activity relationships. *J Med Chem* 51(20):6495–6502. <https://doi.org/10.1021/jm8007486>. <https://doi.org/10.1371/journal.pone.0140113>
13. Ponnusamy S, Halder S, Mulani F, Zinjarde S, Thulasiram H, RaviKumar A (2015) Gedunin and azadiradione: human pancreatic alpha-amylase inhibiting limonoids from neem (*Azadirachta indica*) as anti-diabetic agents. *PLoS ONE* 10(10):e0140113. <https://doi.org/10.1371/journal.pone.0140113>
14. Ferraris FK, Moret KH, Figueredo ABC, Penido C, Maria das Gracas MO (2012) Gedunin, a natural tetranortriterpenoid, modulates T lymphocyte responses and ameliorates allergic inflammation. *Int Immunopharmacol* 14(1):82–93. <https://doi.org/10.1016/j.intimp.2012.06.002>

15. Tharmarajah L, Samarakoon SR, Ediriweera MK et al (2017) In vitro anticancer effect of gedunin on human teratocarcinomal (NTERA-2) cancer stem-like cells. *Hindawi BioMed Res Int* 2017:1–9
16. Subramani R, Gonzalez E, Nandy SB et al (2017) Gedunin inhibits pancreatic cancer by altering sonic hedgehog signaling pathway. *Oncotarget* 8(7):10891–10904
17. Kamath SG, Chen PN, Xiong PY et al (2009) Gedunin, a novel natural substance, inhibits ovarian cancer cell proliferation. *Int J Gynecol cancer* 19(9):1564–1569. <https://doi.org/10.1111/IGC.0b013e3181a83135>
18. Misra S, Verma M, Mishra SK, Srivastava S, Lakshmi V, Misra-Bhattacharya S (2011) Gedunin and photogedunin of *Xylocarpus granatum* possess antifilarial activity against human lymphatic filarial parasite *Brugia malayi* in experimental rodent host. *Parasitol Res* 109(5):1351–1360. <https://doi.org/10.1007/s00436-011-2380-x>
19. Hanahan D, Weinberg RA (2011) Hallmarks of cancer: the next generation. *Cell* 144(5):646–674. <https://doi.org/10.1016/j.cell.2011.02.013>
20. Williams GH, Stoerber K (2012) The cell cycle and cancer. *J Pathol* 226:352–364. <https://doi.org/10.1016/B978-0-12-370458-0.50014-1>
21. Sabharwal SS, Schumacker PT (2014) Mitochondrial ROS in cancer: Initiators, amplifiers or an Achilles' heel? *Nat Rev Cancer* 14(11):709–721. <https://doi.org/10.1038/nrc3803>
22. Elmore S, Apoptosis (2007) A review of programmed cell death. *Toxicol Pathol* 35(4):495–516. <https://doi.org/10.1080/01926230701320337>
23. Skehan P, Storeng R, Scudiero D et al (1990) New colorimetric cytotoxicity assay for anticancer-drug screening. *J Natl Cancer Inst* 82(13):1107–1112. <https://doi.org/10.1093/jnci/82.13.1107>
24. Liang CC, Park AY, Guan JL (2007) In vitro scratch assay: a convenient and inexpensive method for analysis of cell migration in vitro. *Nat Protoc* 2(2):329–333. <https://doi.org/10.1038/nprot.2007.30>
25. Riccardi C, Nicoletti I (2006) Analysis of apoptosis by propidium iodide staining and flow cytometry. *Nat Protoc* 1(3):1458–1461. <https://doi.org/10.1038/nprot.2006.238>
26. Hasanain M, Sahai R, Pandey P et al (2020) Microtubule disrupting agent-mediated inhibition of cancer cell growth is associated with blockade of autophagic flux and simultaneous induction of apoptosis. *Cell Prolif* 53(4):e12749. <https://doi.org/10.1111/cpr.12749>
27. Kathuria M, Bhattacharjee A, Sashidhara KV, Singh SP, Mitra K (2014) Induction of mitochondrial dysfunction and oxidative stress in leishmania donovani by orally active clerodane diterpene. *Antimicrob Agents Chemother* 58(10):5916–5928. <https://doi.org/10.1128/AAC.02459-14>
28. Vermes I, Haanen C, Steffens-Nakken H, Reutelingsperger C (1995) A novel assay for apoptosis flow cytometric detection of phosphatidylserine expression on early apoptotic cells using fluorescein labelled Annexin V. *J Immunol Methods* 184(1):39–51. [https://doi.org/10.1016/0022-1759\(95\)00072-1](https://doi.org/10.1016/0022-1759(95)00072-1)
29. Bhattacharjee A, Hasanain M, Kathuria M, Singh A (2018) Ormeloxifene-induced unfolded protein response contributes to autophagy-associated apoptosis via disruption of Akt/mTOR and activation of JNK. *Sci Rep* 8(2303):1–13. <https://doi.org/10.1038/s41598-018-20541-8>
30. DiPaola RS (2002) To arrest or not to G2-M cell-cycle arrest. *Clin Cancer Res* 8(November):3311–3314
31. Ando T, Kawabe T, Ohara H, Ducommun B, Itoh M, Okamoto T (2001) Involvement of the interaction between p21 and proliferating cell nuclear antigen for the maintenance of G 2/M arrest after DNA damage. *J Biol Chem* 276(46):42971–42977. <https://doi.org/10.1074/jbc.M106460200>
32. Sakaguchi K, Herrera JE, Saito S et al (1998) DNA damage activates p53 through a phosphorylation—acetylation cascade. *Genes Dev* 12:2831–2841
33. Sharma A, Singh K, Almasan A (2012) Histone H2AX phosphorylation: a marker for DNA damage. In: *DNA repair protocols*. Methods in Springer, pp 1–11. https://doi.org/10.1007/978-1-61779-998-3_40
34. Zorova LD, Popkov VA, Plotnikov EY et al (2018) Mitochondrial membrane potential. *Anal Biochem* 552:50–59. <https://doi.org/10.1016/j.ab.2017.07.009>
35. Tait SWG, Green DR (2013) Mitochondrial regulation of cell death. *Cold Spring Harb Perspect Biol* 5:75–90. <https://doi.org/10.1101/cshperspect.a008706>
36. Tait SWG, Green DR (2010) Mitochondria and cell death: outer membrane permeabilization and beyond. *Nat Rev Mol Cell Biol* 11(9):621–632. <https://doi.org/10.1038/nrm2952>
37. Morrison DK (2012) MAP kinase pathways. *Cold Spring Harb Perspect Biol* 4(11):a011254
38. Liu J, Lin A (2005) Role of JNK activation in apoptosis: a double-edged sword. *Cell Res* 15(1):36–42
39. <https://www.picard.ch/downloads/Hsp90interactors.pdf>. Hsp90 Interactors
40. Wang J, Luo B, Li X et al (2017) Inhibition of cancer growth in vitro and in vivo by a novel ROS-modulating agent with ability to eliminate stem-like cancer cells. *Cell Death Dis* e2887:1–9. <https://doi.org/10.1038/cddis.2017.272>
41. Trepel J, Mollapour M, Giaccone G, Neckers L (2010) Targeting the dynamic HSP90 complex in cancer. *Nat Rev Cancer* 10(8):537–549. <https://doi.org/10.1038/nrc2887>
42. Williams AB, Schumacher B (2016) p53 in the DNA-damage-repair process. *Cold Spring Harb Perspect Med* 6(5):1–16. <https://doi.org/10.1101/cshperspect.a026070>
43. Wang Z, Yu K, Hu Y et al (2019) Schisantherin A induces cell apoptosis through ROS/JNK signaling pathway in human gastric cancer cells. *Biochem Pharmacol* 173:113673. <https://doi.org/10.1016/j.bcp.2019.113673>
44. Liu L, Zhu H, Wu W et al (2019) Neoantimycin F, a streptomycetes—derived natural product induces mitochondria-related apoptotic death in human non-small cell lung cancer cells. *Front Pharmacol* 10(September):1–13. <https://doi.org/10.3389/fphar.2019.01042>
45. Zhang X, Jiang J, Chen Z, Cao M (2019) Silibinin inhibited autophagy and mitochondrial apoptosis in pancreatic carcinoma by activating JNK / SAPK signaling. *Pathol Res Pract* 215(9):152530. <https://doi.org/10.1016/j.prp.2019.152530>
46. Wang J, Shen G, Luo Y et al (2019) 2-(4-methoxyphenylthio)-5,8-dimethoxy-1,4-naphthoquinone induces apoptosis via ROS mediated MAPK and STAT3 signaling pathway in human gastric cancer cells. *J Chemother* 31(4):214–226. <https://doi.org/10.1080/1120009X.2019.1610832>
47. Liu C, Shen G-N, Luo Y-H et al (2020) Novel 1,4-naphthoquinone derivatives induce apoptosis via ROS-mediated p38/MAPK, Akt and STAT3 signaling in human hepatoma Hep3B cells. *Int J Biochem Cell Biol* 96:9–19
48. Basu S, Rajakaruna S, Reyes B et al (2014) Suppression of MAPK/JNK-MTORC1 signaling leads to premature loss of organelles and nuclei by autophagy during terminal differentiation of lens fiber cells. *Autophagy* 10(7):1193–1211. <https://doi.org/10.4161/auto.28768>
49. Cuyàs E, Corominas-Faja B, Joven J, Menendez JA (2014) Cell cycle regulation by the nutrient-sensing mammalian target of rapamycin (mTOR) Pathway. In: *Cell cycle control, methods in molecular biology (methods and protocols)*. vol 1170. Humana Press, New York, pp 113–144

50. Ha G-H, Park J-S, Breuer E-KY (2013) TACC3 promotes epithelial-mesenchymal transition (EMT) through the activation of PI3K/Akt and ERK signaling pathways. *Cancer Lett* 332(1):63–73
51. Kim S, Kim K, Park S et al (2017) Mitochondrial ROS activates ERK/autophagy pathway as a protected mechanism against deoxypodophyllotoxin-induced apoptosis. *Oncotarget* 8(67):111581–111596
52. Santucci R, Sinibaldi F, Cozza P, Polticelli F, Fiorucci L (2019) Cytochrome c: an extreme multifunctional protein with a key role in cell fate. *Int J Biol Macromol* 136:1237–1246. <https://doi.org/10.1016/j.ijbiomac.2019.06.180>
53. Shen HM, Liu ZG (2006) JNK signaling pathway is a key modulator in cell death mediated by reactive oxygen and nitrogen species. *Free Radic Biol Med* 40(6):928–939. <https://doi.org/10.1016/j.freeradbiomed.2005.10.056>
54. Chambers JW, LoGrasso PV (2011) Mitochondrial c-Jun N-terminal Kinase (JNK) signaling initiates physiological changes resulting in amplification of reactive oxygen species generation. *J Biol Chem* 286(18):16052–16062. <https://doi.org/10.1074/jbc.M111.223602>
55. Tsuruta F, Sunayama J, Mori Y et al (2004) JNK promotes Bax translocation to mitochondria through phosphorylation of 14-3-3 proteins. *EMBO J* 23(8):1889–1899. <https://doi.org/10.1038/sj.emboj.7600194>
56. Whitesell L, Lindquist SL (2005) HSP90 and the chaperoning. *Nat Rev Cancer* 5:761–772. <https://doi.org/10.1038/nrc1716>
57. Gaspar N, Sharp SY, Eccles SA et al (2010) Mechanistic evaluation of the novel HSP90 inhibitor NVP-AUY922 in adult and pediatric glioblastoma. *Mol Cancer Ther* 9(5):1219–1233. <https://doi.org/10.1158/1535-7163.MCT-09-0683>
58. Nagaraju GP, Mezina A, Shaib WL, Landry J, El-Rayes BF (2016) Targeting the Janus-activated kinase-2-STAT3 signalling pathway in pancreatic cancer using the HSP90 inhibitor ganetespib. *Eur J Cancer* 52:109–119. <https://doi.org/10.1016/j.ejca.2015.10.057>
59. Boridy S, Le PU, Petrecca K, Maysinger D (2014) Celastrol targets proteostasis and acts synergistically with a heat-shock protein 90 inhibitor to kill human glioblastoma cells. *Cell Death Dis* 5(e1216):1–12. <https://doi.org/10.1038/cddis.2014.182>
60. Zhang Z, Miao L, Lv C et al (2013) Wentilactone B induces G2/M phase arrest and apoptosis via the Ras/Raf/MAPK signaling pathway in human hepatoma SMMC-7721 cells. *Cell Death Dis* 4(6):e657. <https://doi.org/10.1038/cddis.2013.182>
61. Rouf R, Uddin SJ, Shilpi JA, Alamgir M (2007) Assessment of antidiarrhoeal activity of the methanol extract of *Xylocarpus granatum* bark in mice model. *J Ethnopharmacol* 109(3):539–542. <https://doi.org/10.1016/j.jep.2006.08.015>

Publisher's Note Springer Nature remains neutral with regard to jurisdictional claims in published maps and institutional affiliations.